

# T-count and Qubit Optimized Quantum Circuit Design of the Non-Restoring Square Root Algorithm

EDGARD MUÑOZ-COREAS AND HIMANSHU THAPLIYAL, University of Kentucky, USA

Quantum circuits for basic mathematical functions such as the square root are required to implement scientific computing algorithms on quantum computers. Quantum circuits that are based on Clifford+T gates can be made fault tolerant in nature but the T gate is very costly to implement. As a result, reducing T-count has become an important optimization goal. Further, quantum circuits with many qubits are difficult to realize making designs that save qubits and produce no garbage outputs desirable. In this work, we present a T-count optimized quantum square root circuit with only  $2 \cdot n + 1$  qubits and no garbage output. To have fair comparison against existing work, the Bennett's garbage removal scheme is used to remove garbage output from existing works. We determined that the proposed design achieves an average T-count savings of 40.91%, 98.88%, 39.25% and 26.11% as well as qubit savings of 85.46%, 95.16%, 90.59% and 86.77% compared to existing work.

CCS Concepts: • **Hardware** → **Quantum computation**; *Emerging architectures*; Arithmetic and datapath circuits;

Additional Key Words and Phrases: Quantum arithmetic circuit, Quantum gate, Non-restoring division, Resource optimization

## ACM Reference Format:

Edgard Muñoz-Coreas and Himanshu Thapliyal. 2010. T-count and Qubit Optimized Quantum Circuit Design of the Non-Restoring Square Root Algorithm. *ACM J. Emerg. Technol. Comput. Syst.* 9, 4, Article 39 (March 2010), 19 pages. <https://doi.org/0000001.0000001>

## 1 INTRODUCTION

Among the emerging computing paradigms, quantum computing appears to be promising due to its applications in number theory, encryption, search and scientific computation [7] [4] [16] [24] [20] [23]. Quantum circuits for arithmetic operations such as addition, multiplication, square root and fractional powers are required in the quantum circuit implementations of many quantum algorithms in these areas [9] [4] [6] [7]. The design of quantum circuits for arithmetic operations such as addition and multiplication have received notable attention in the literature. However, the design of the quantum circuits for crucial arithmetic functions such as the square root is still at an initial stage.

Reliable quantum circuits must be able to tolerate noise errors [25] [26] [17] [19]. Fault tolerant quantum gates (such as Clifford+T gates) and quantum error correcting codes can be used to make quantum circuits resistant to noise errors [1] [14] [2] [12] [18] [8]. However, the increased tolerance to noise errors comes with the increased implementation overhead associated with the quantum T gate [1] [18] [27] [8]. Because of the increased cost to realize the T gate, T-count has become an

---

Author's address: Edgard Muñoz-Coreas and Himanshu Thapliyal, University of Kentucky, Department of Electrical and Computer Engineering, Lexington, KY, 40506, USA, [hthapliyal@uky.edu](mailto:hthapliyal@uky.edu).

---

Permission to make digital or hard copies of all or part of this work for personal or classroom use is granted without fee provided that copies are not made or distributed for profit or commercial advantage and that copies bear this notice and the full citation on the first page. Copyrights for components of this work owned by others than the author(s) must be honored. Abstracting with credit is permitted. To copy otherwise, or republish, to post on servers or to redistribute to lists, requires prior specific permission and/or a fee. Request permissions from [permissions@acm.org](mailto:permissions@acm.org).

© 2009 Copyright held by the owner/author(s). Publication rights licensed to Association for Computing Machinery.  
1550-4832/2010/3-ART39 \$15.00  
<https://doi.org/0000001.0000001>

important performance measure for fault tolerant quantum circuit design [1] [10]. Further, existing quantum computers have few qubits and large-scale quantum computers are difficult to realize [11] [15]. As a result, the total number of qubits required by a quantum circuit is an important performance measure. Quantum circuits have overhead called ancillae and garbage output that adds to the total number of qubits of a quantum circuit. Any constant inputs in the quantum circuit are called ancillae. Garbage output exist in the quantum circuit to preserve one-to-one mapping. Garbage output are not primary inputs or useful outputs. Minimizing the overhead from ancillae and garbage output is a means to reduce overall qubit cost of a quantum circuit.

The design of quantum circuits for the calculation of the square root has only recently begun to be addressed in the literature. A design for the calculation of the square root based on the Newton approximation algorithm is presented in [6]. While an interesting design, the implementation requires  $5 \cdot \lceil \log_2(n) \rceil$  multiplications and  $3 \cdot \lceil \log_2(n) \rceil$  additions (where  $n$  is the accuracy of the solution and  $n \geq 4$ ) [6]. This arithmetic operation cost translates into significant T gate and qubit cost. The recent design in [21] presents a quantum circuit for calculating the square root based on the non-restoring square root algorithm. The recent design in [21] requires only  $\frac{n}{2}$  additions or subtractions making the design far more efficient than the design in [6] in terms of qubits and T gates. However, the design in [21] does not include the additional ancillae and T gate costs from removing garbage outputs. Additional recent quantum circuit designs for calculating the square root presented in [3] also require only  $\frac{n}{2}$  controlled subtraction operations. The designs in [3] are based on the non-restoring square root algorithm. Thus, the designs presented in [3] also offer more efficient alternatives to the design in [6] in terms of qubits and T gates. One of the designs presented in [3] has been optimized for gate count further reducing its T-gate cost. In this design, where possible, portions of the circuitry that implements the controlled subtraction operations are replaced by quantum circuit modules that require fewer gates. The amount of optimization possible depended on what inputs to the controlled subtraction circuitry, if any, could be assumed constant. Both designs presented in [3] produce significant garbage output. The qubit and T gate cost associated with removing this garbage output was not considered in the circuit cost calculations reported in [3] for both designs. Thus, while significant improvements, the quantum square root circuits in [21] and [3] still have significant overhead in terms of T-count and qubits. *To overcome the limitations of existing designs, we present the design of a quantum square root circuit that is garbageless, requires  $2 \cdot n + 1$  qubits and is optimized for T-count.* The quantum square root circuit based on our proposed design is compared and is shown to be better than the existing designs of quantum square root circuit in terms of both T-count and qubits.

This paper is organized as follows: Section 2 presents background information on the Clifford+T gates. In section 3 we present an overview of the proposed quantum square root circuit. In section 4 we present the design methodology to implement our proposed quantum square root circuit. In section 5 we prove the correctness of our design and in section 6 our proposed design is compared to the existing work.

## 2 BACKGROUND

### 2.1 Fault Tolerant Quantum Circuits

The fault tolerant Clifford+T gate set is used in fault tolerant quantum circuit design. Table 1 shows the gates that make up the Clifford+T gate set. *The quantum square root circuit proposed in this work is composed of the quantum NOT gate, Feynman (CNOT) gate, inverted control CNOT gate, SWAP gate and Toffoli gate.* Table 1 illustrates that the CNOT gate and NOT gates are Clifford+T gates. The Clifford+T implementation of the inverted control CNOT gate, SWAP gate and Toffoli gate are shown in figure 1. In this work, we use the Clifford+T Toffoli gate implementation presented in

Table 1. The Clifford + T gates

Type of Gate	Symbol	Matrix
NOT gate	$N$	$\begin{bmatrix} 0 & 1 \\ 1 & 0 \end{bmatrix}$
Hadamard gate	$H$	$\frac{1}{\sqrt{2}} \begin{bmatrix} 1 & 1 \\ 1 & -1 \end{bmatrix}$
$T$ gate	$T$	$\begin{bmatrix} 1 & 0 \\ 0 & e^{i \cdot \frac{\pi}{4}} \end{bmatrix}$
$T$ gate Hermitian transpose	$T^\dagger$	$\begin{bmatrix} 1 & 0 \\ 0 & e^{-i \cdot \frac{\pi}{4}} \end{bmatrix}$
Phase gate	$S$	$\begin{bmatrix} 1 & 0 \\ 0 & i \end{bmatrix}$
Phase gate Hermitian transpose	$S^\dagger$	$\begin{bmatrix} 1 & 0 \\ 0 & -i \end{bmatrix}$
CNOT gate	$C$	$\begin{bmatrix} 1 & 0 & 0 & 0 \\ 0 & 1 & 0 & 0 \\ 0 & 0 & 0 & 1 \\ 0 & 0 & 1 & 0 \end{bmatrix}$

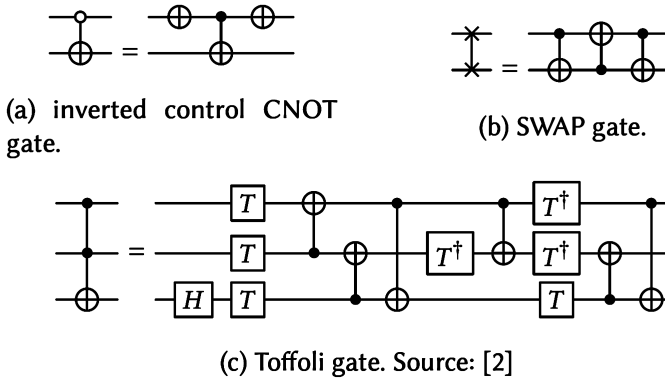


Fig. 1. The fault tolerant Clifford + T implementations of quantum logic gates used in this work.

[2]. The inverted control CNOT gate and the SWAP gate are 2 input, 2 output logic gates that have the mapping  $A, B$  to  $A, \bar{A} \oplus B$  and  $A, B$  to  $B, A$  respectively. The Toffoli gate is a 3 input, 3 output logic gate and has the mapping  $A, B, C$  to  $A, B, A \cdot B \oplus C$ .

Fault tolerant quantum circuit performance is evaluated in terms of T-count because the implementation costs of the T gate is significantly greater than the implementation costs of the other Clifford+T gates [1] [18] [27] [8] [10]. *T-count is the total number of T gates or Hermitian transposes of the T gate in a quantum circuit.* As illustrated in figure 1, the inverted control CNOT gate and the SWAP gate both have a T-count of 0 while the Toffoli gate has a T-count of 7.

### 3 OVERVIEW OF PROPOSED QUANTUM SQUARE ROOT CIRCUIT

We now present the design of our proposed quantum square root circuit. The proposed quantum square root circuit has the mapping  $|A\rangle, |B\rangle, |Z\rangle$  to  $|Remainder\rangle, |\sqrt{A}\rangle, |Z\rangle$  where  $|B\rangle$  is initialized

to 1 and  $|Z\rangle$  is initialized to 0. The proposed method is garbageless and requires fewer qubits than existing designs. The proposed method also has a lower T-count compared to existing designs.

Consider the square root of a 2's complement positive binary number  $a$  of even bit length  $n$ . At the end of computation, the non-restoring square root algorithm returns  $\sqrt{a}$  and the remainder  $r$  of the calculation of the square root. The non-restoring square root algorithm is illustrated in figure 2.

---

**Algorithm 1: Non-restoring square root algorithm**

---

```

Function Non-Restoring( $a$ )
  {
    /* START PART 1 */
     $r = 1$ ;
     $r_{n-1:n-2} = r_{n-1:n-2} - 1$ ;
     $\sqrt{a_{\frac{n}{2}-1}} = r_{n-1}$ ;
    /* END PART 1 */
    For  $i = 2$  to  $\frac{n}{2} - 1$ 
      /* START PART 2 */
      If ( $r < 0$ )
         $r_{n-1:n-2:i} = r_{n-1:n-2:i} + (\sqrt{a} \cdot 4 + 3)$ ;
         $\sqrt{a_{\frac{n}{2}-i}} = r_{n-1}$ ;
      Else
         $r_{n-1:n-2:i} = r_{n-1:n-2:i} - (\sqrt{a} \cdot 4 + 1)$ ;
         $\sqrt{a_{\frac{n}{2}-i}} = r_{n-1}$ ;
      End
    /* END PART 2 */
    End
    /* START PART 3 */
    If ( $r < 0$ )
       $r_{n-1:0} = r_{n-1:0} + (\sqrt{a} \cdot 4 + 3)$ ;
       $\sqrt{a_0} = r_{n-1}$ ;
       $r = r + (\sqrt{a} \cdot 4 + 1)$ ;
    Else
       $r_{n-1:0} = r_{n-1:0} - (\sqrt{a} \cdot 4 + 1)$ ;
       $\sqrt{a_0} = r_{n-1}$ ;
    End
    /* END PART 3 */
    Return:  $r, \sqrt{a}$ ;
  }

```

---

Fig. 2. The Non-restoring square root algorithm. The portions of the algorithm completed by each Part of the proposed quantum square root circuit are shown.

The proposed quantum square root circuit is divided into three parts: (i) Part 1: Initial Subtraction, (ii) Part 2: Conditional Addition or Subtraction and (iii) Part 3: Remainder Restoration. Figure 2 illustrates how each Part implements the non-restoring square root algorithm. Parts 1 and 3 are only applied once while Part 2 will be iterated a total of  $\frac{n}{2} - 2$  times. Figure 3 shows a generic example of the quantum implementation of the algorithm in figure 2.

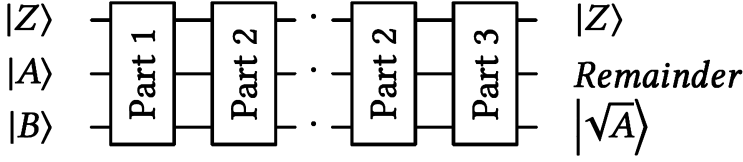


Fig. 3. Example of the complete proposed square root circuit.

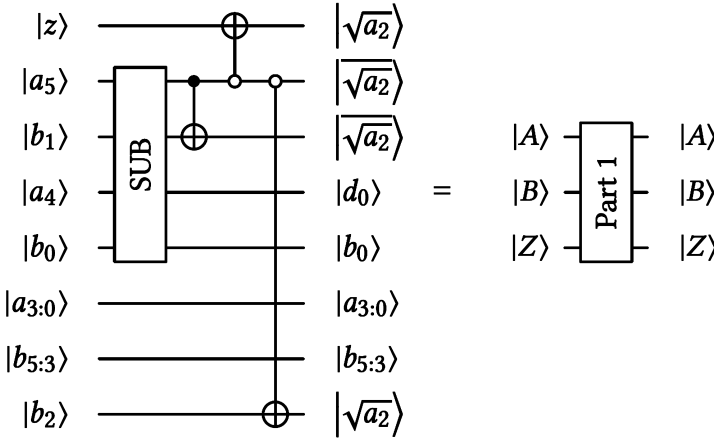


Fig. 4. Circuit generation of Part 1 of the proposed quantum square root circuit. Quantum circuit and graphical representation are shown.

A quantum circuit is generated for each Part of the design. Figure 4 illustrates the quantum circuit implementation of Part 1 for the calculation of the square root for a 6 bit number  $a_5 \dots a_0$ . The quantum circuit takes the quantum registers  $|A\rangle$ ,  $|B\rangle$  and  $|z\rangle$  as inputs. At the end of computation, the value  $\sqrt{a_{\frac{n}{2}-1}}$  appears at location  $|A_{n-1}\rangle$ . This value is calculated by the quantum subtraction circuit (the quantum subtraction circuit is labeled SUB in figure 4). The value  $\sqrt{a_{\frac{n}{2}-1}}$  corresponds to the most significant difference bit ( $d_1$ ) from the subtraction of quantum register locations  $|A_{n-1:n-2}\rangle$  and  $|B_{1:0}\rangle$ . The remaining quantum gates serve to perform the transformations necessary to prepare quantum register  $|B\rangle$  for the calculation of the next bit of the square root of  $a$ . Register location  $|B_1\rangle$  is transformed based on the value of  $\sqrt{a_{\frac{n}{2}-1}}$  and  $\sqrt{a_{\frac{n}{2}-1}}$  is placed at location  $|B_2\rangle$ .  $|z\rangle$  is transformed to  $\sqrt{a_{\frac{n}{2}-1}}$ . The value on  $|z\rangle$  will be used in subsequent computation.

Figure 5 illustrates the quantum circuit implementation of Part 2 for the calculation of the square root for a 6 bit number  $a_5 \dots a_0$ . Part 2 is repeated a total of  $\frac{n}{2} - 2$  times. The quantum circuit takes the output of either Part 1 or a previous iteration of Part 2 as inputs. At the end of computation, the value  $\sqrt{a_i}$  of the square root will appear at quantum register location  $|A_{n-1}\rangle$  where  $1 \leq i \leq \frac{n}{2} - 2$ . The value  $\sqrt{a_i}$  corresponds to the most significant result bit  $d_{1+2 \cdot i}$  from the conditional addition or subtraction of quantum registers  $|A_{n-1:n-2-2 \cdot i}\rangle$  and  $|B_{1+2 \cdot i:0}\rangle$  where  $1 \leq i \leq \frac{n}{2} - 2$ . The conditional addition or subtraction is performed by a quantum conditional addition or subtraction (ADD/SUB) circuit conditioned on the value in quantum register  $|z\rangle$ . Garbageless quantum ADD/SUB circuits encountered in the literature such as the design in [22] perform addition when the control qubit

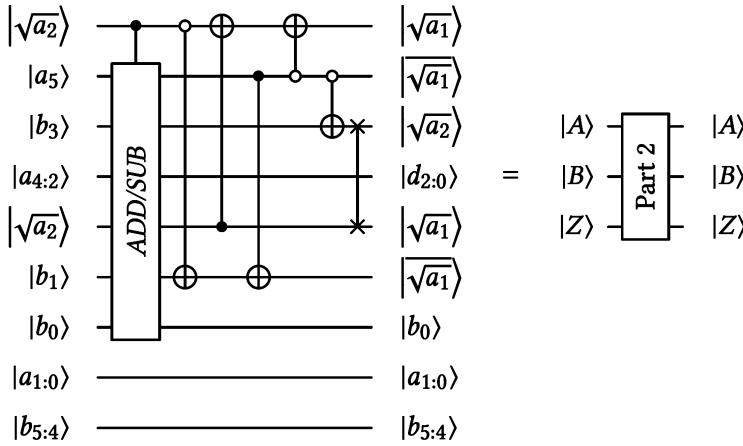


Fig. 5. Circuit generation of Part 2 of the proposed quantum square root circuit. Quantum circuit and graphical representation are shown.

$ctrl = 0$  and subtraction when  $ctrl = 1$ . Our design assumes a quantum *ADD/SUB* circuit that behaves identical to designs proposed in existing works such as [22]. The remaining quantum gates prepare the quantum registers  $|B\rangle$  and  $|z\rangle$  for the next round of computation. Quantum register locations  $|z\rangle$  and  $|b_1\rangle$  are first restored to their initial values then transformed again based on the value  $\sqrt{a_i}$ . The square root value  $\sqrt{a_i}$  is copied to quantum register location  $|B_{2.i+2}\rangle$ . The quantum swap gates reorder the positions of  $\sqrt{a}$  on quantum register  $|B\rangle$  such that the values are in descending order with the most significant bit of  $\sqrt{a}$  occupying quantum register location  $|B_{2.i+2}\rangle$ , the next significant value of  $\sqrt{a}$  occupying quantum register location  $|B_{2.i+1}\rangle$  and so forth. The calculated digits of  $\sqrt{a}$  must be in descending order for the next round of computation.

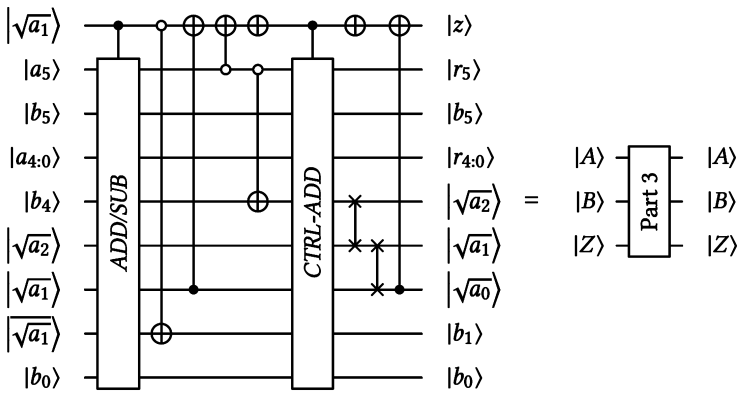


Fig. 6. Circuit generation of Part 3 of the proposed quantum square root circuit. Quantum circuit and graphical representation are shown.

Figure 6 illustrates the quantum circuit implementation of Part 3. The circuit takes the results of the final iteration of Part 2 as inputs. At the end of computation, the  $\sqrt{a}$  will appear at quantum

register locations  $\left|B_{\frac{n}{2}+2:2}\right\rangle$ . The remainder from calculating square root of  $a$  will appear at quantum register  $|A\rangle$  and quantum register  $|z\rangle$  will be restored to the value 0. All other locations in quantum register  $|B\rangle$  will also be restored to their initial values. The purpose of the quantum *ADD/SUB* circuit is to produce the final digit of the square root ( $\sqrt{a_0}$ ). The value  $\sqrt{a_0}$  corresponds to the most significant difference bit from the conditional addition or subtraction of quantum registers  $|A\rangle$  and  $|B\rangle$ . The four CNOT and inverted control CNOT gates that immediately follow the quantum *ADD/SUB* circuit restore quantum registers  $|B_1\rangle$  and  $|z\rangle$  to their original values and then transform the value in register  $|z\rangle$  based on the value  $\sqrt{a_0}$ . The value  $\sqrt{a_0}$  is also copied to quantum register location  $\left|B_{\frac{n}{2}+2}\right\rangle$  as well. The purpose of the quantum conditional addition (*CTRL-ADD*) circuit is to restore the remainder from calculating  $\sqrt{a}$ . The quantum *CTRL-ADD* circuit is conditioned on the value in quantum register  $|z\rangle$ . Garbageless quantum *CTRL-ADD* circuits encountered in the literature such as the design in [13] perform addition when the control qubit  $ctrl = 0$  and perform no operation when  $ctrl = 1$ . Our design assumes a quantum *CTRL-ADD* circuit that behaves identical to designs proposed in existing works such as [13]. Thus, if the result of the quantum *ADD/SUB* circuit turns out to be negative, the quantum *CTRL-ADD* circuit will perform addition. Therefore, at the end of computation, the quantum register  $|A\rangle$  will always hold a positive value representing the remainder from calculating  $\sqrt{a}$ . The quantum not gates on  $|z\rangle$  preceding and following the quantum *CTRL-ADD* circuit are required to ensure correct operation of the quantum *CTRL-ADD* circuit and to restore  $|z\rangle$  to its original value. The quantum swap gates reorder the positions of  $\sqrt{a}$  on quantum register  $|B\rangle$  such that the values are in descending order with the most significant bit of  $\sqrt{a}$  occupying quantum register location  $\left|B_{\frac{n}{2}+2}\right\rangle$ , the next significant value of  $\sqrt{a}$  occupying quantum register location  $\left|B_{\frac{n}{2}+1}\right\rangle$  and so forth. Thus, the  $\sqrt{a}$  will appear in descending bit order at quantum register locations  $\left|B_{\frac{n}{2}+2:2}\right\rangle$ . The CNOT gate after the swap gates completes the restoration of  $|z\rangle$  to the value 0.

#### 4 DESIGN METHODOLOGY OF THE PROPOSED QUANTUM SQUARE ROOT CIRCUIT

In this section, detailed steps outlining the proposed design methodology are explained for each Part of the proposed square root circuit. The steps involved in the proposed methodology are explained for calculating the square root of the number  $a$ . Illustrative examples of the generated circuits of each Part of the square root circuit are shown. The illustrated quantum circuits show the generation of a quantum circuit that calculates the square root of a six bit, positive and 2's complement binary number  $a = a_5 \dots a_0$ . The state transformations on quantum registers  $|A\rangle$ ,  $|B\rangle$  and  $|z\rangle$  are also shown. Figure 7 illustrates the generation of Part 1 and figures 8 and 9 illustrate the generation of Part 2. Figures 10 and 11 illustrate the generation of Part 3.

##### 4.1 Part 1: Initial Subtraction

This Part is only repeated once. There are 5 Steps in this Part.

- Step 1: For  $i = 0$  to 1:  
At pair of locations  $|a_{n-1-i}\rangle$  and  $|b_i\rangle$  apply the quantum subtraction circuit such that the location  $|b_i\rangle$  will maintain the same value while location  $|a_{n-1-i}\rangle$  is transformed to the difference bit  $|d_{1-i}\rangle$ .
- Step 2: At locations  $|a_{n-1}\rangle$  and  $|b_1\rangle$  apply a CNOT gate such that the location  $|a_{n-1}\rangle$  will maintain the same value while location  $|b_1\rangle$  transforms to  $|d_1 \oplus b_1\rangle$ .

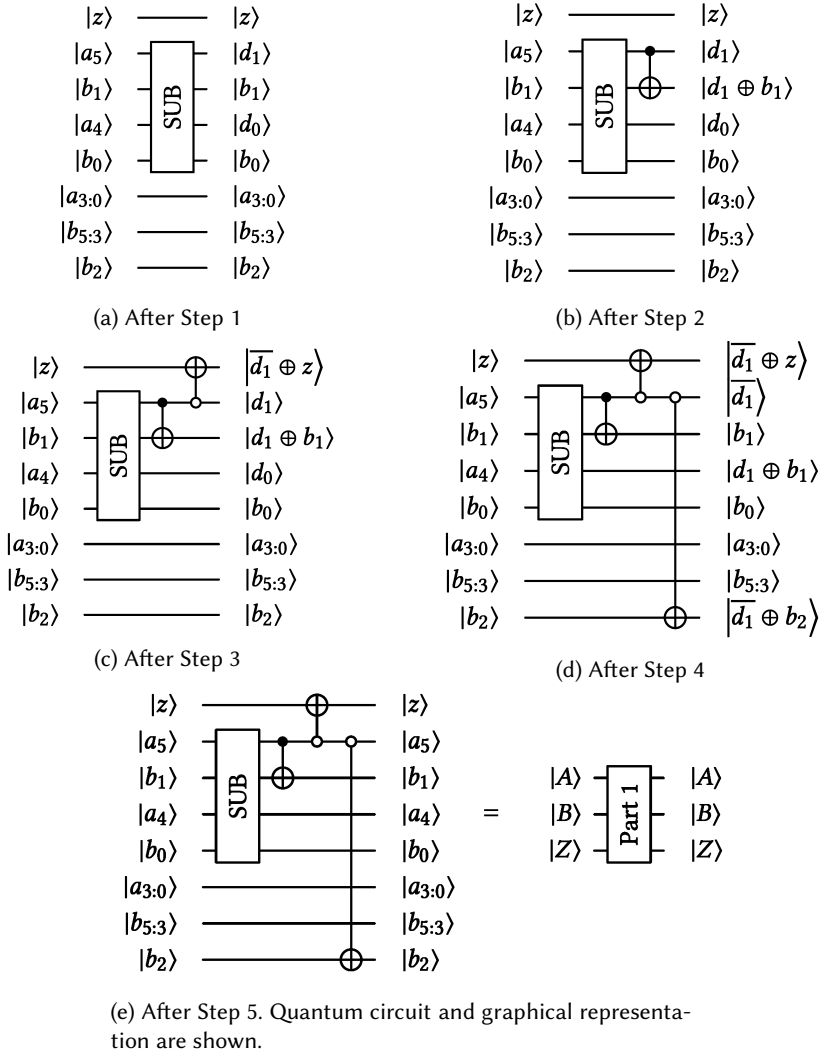


Fig. 7. Circuit generation of Part 1 of the proposed quantum square root circuit: Steps 1-5.

- Step 3: At locations  $|a_{n-1}\rangle$  and  $|z\rangle$  apply an inverted control CNOT gate such that the location  $|a_{n-1}\rangle$  will maintain the same value while location  $|z\rangle$  transforms to  $|d_1 \oplus z\rangle$ .
- Step 4: At locations  $|a_{n-1}\rangle$  and  $|b_2\rangle$  apply an inverted control CNOT gate such that the location  $|a_{n-1}\rangle$  will maintain the same value while location  $|b_2\rangle$  transforms to  $|\overline{d_1} \oplus b_2\rangle$ .
- Step 5: Step 5 has the following two sub-steps
  - Step 1: For  $i = 0$  to 1:
    - Reassign the names of the value stored in the location with the value  $|d_i\rangle$  to the name  $|a_{n-1-(1-i)}\rangle$
  - Step 2: Reassign the names of the values stored in the locations  $|b_2\rangle$ ,  $|b_1\rangle$  and  $|z\rangle$  to the names  $b_2$ ,  $b_1$  and  $z$  respectively.



4.2 Part 2: Conditional Addition or Subtraction

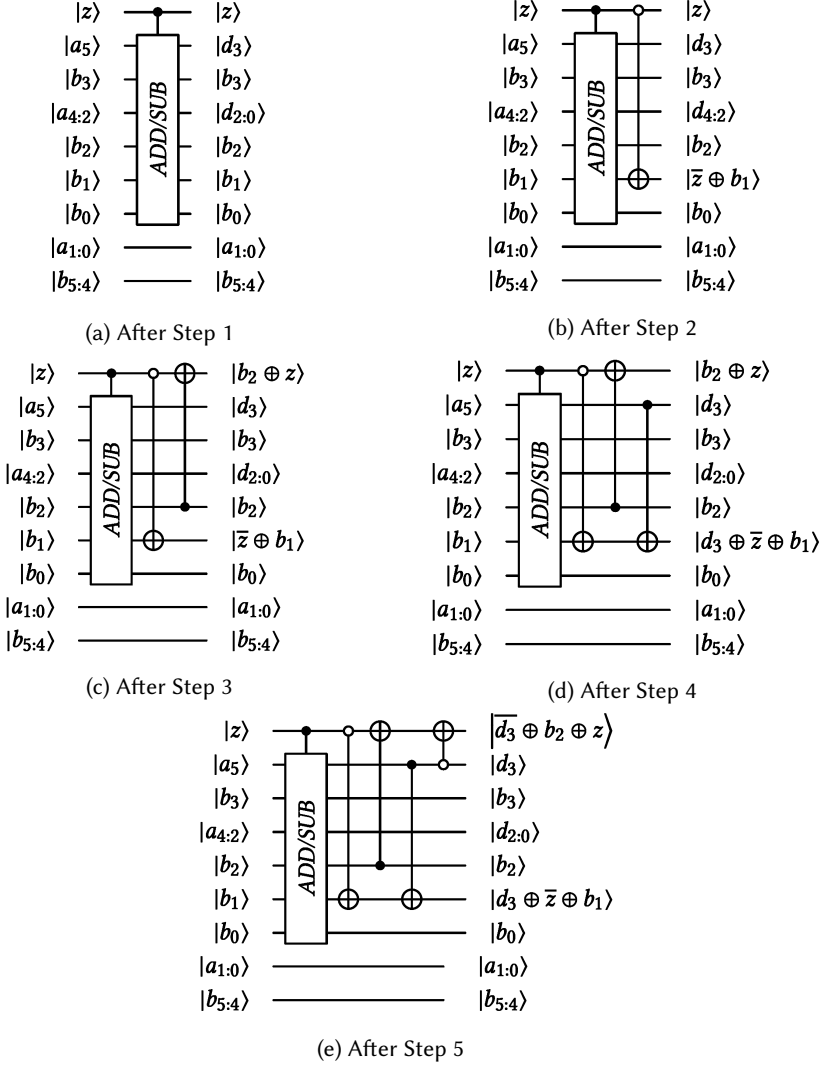


Fig. 8. Circuit generation of Part 2 of the proposed quantum square root circuit: Steps 1-5.

This Part is repeated  $\frac{n}{2} - 2$  times. There are 8 steps in this Part. For  $i = 2$  to  $\frac{n}{2} - 1$ :

- Step 1: this Step has two sub-steps.
  - Step 1: For  $j = 0$  to  $2 \cdot i - 1$ :  
At pair of locations  $|a_{n-1-j}\rangle$  and  $|b_j\rangle$  apply the quantum conditional addition or subtraction (ADD/SUB) circuit such that location  $|b_j\rangle$  will maintain the same value while location  $|a_{n-1-j}\rangle$  transforms to the sum or difference bit  $|d_{2 \cdot i - j - 1}\rangle$ .
  - Step 2: At location  $|z\rangle$  apply the quantum ADD/SUB circuit such that the operation of the ADD/SUB circuit will be conditioned on the value at location  $|z\rangle$

- Step 2: At locations  $|z\rangle$  and  $|b_1\rangle$  apply an inverted control CNOT gate such that the location  $|z\rangle$  will maintain the same value while location  $|b_1\rangle$  transforms to  $|\bar{z} \oplus b_1\rangle$ .
- Step 3: At locations  $|b_2\rangle$  and  $|z\rangle$  apply a CNOT gate such that the location  $|b_2\rangle$  will maintain the same value while location  $|z\rangle$  transforms to  $|b_2 \oplus z\rangle$ .

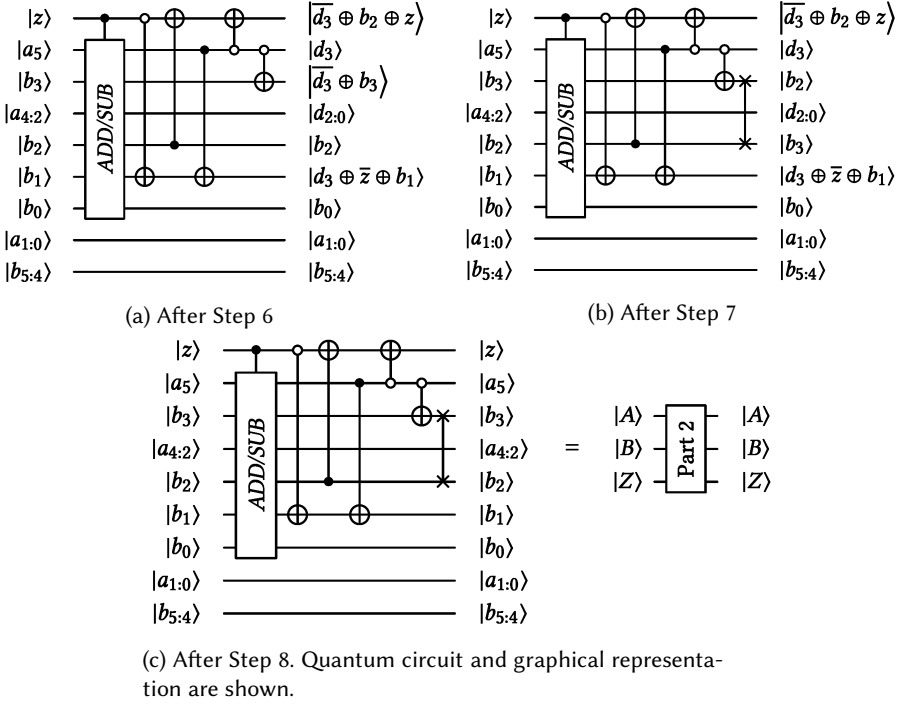


Fig. 9. Circuit generation of Part 2 of the proposed quantum square root circuit: Steps 6-8.

- Step 4: At locations  $|a_{n-1}\rangle$  and  $|b_1\rangle$  apply a CNOT gate such that the location  $|a_{n-1}\rangle$  will maintain the same value while location  $|b_1\rangle$  transforms to  $|d_{2,i-1} \oplus z \oplus b_1\rangle$ .
- Step 5: At locations  $|a_{n-1}\rangle$  and  $|z\rangle$  apply an inverted control CNOT gate such that the location  $|a_{n-1}\rangle$  will maintain the same value while location  $|z\rangle$  transforms to  $|\overline{d_{2,i-1}} \oplus b_2 \oplus z\rangle$ .
- Step 6: At locations  $|a_{n-1}\rangle$  and  $|b_{i+1}\rangle$  apply an inverted control CNOT gate such that the location  $|a_{n-1}\rangle$  will maintain the same value while location  $|b_{i+1}\rangle$  transforms to  $|\overline{d_{2,i-1}} \oplus b_{i+1}\rangle$ .
- Step 7: For  $j = i + 1$  to 3:  
At locations  $|b_j\rangle$  and  $|b_{j-1}\rangle$  apply a quantum SWAP gate such that location  $|b_j\rangle$  will have the value at location  $|b_{j-1}\rangle$  and location  $|b_{j-1}\rangle$  will have the value at location  $|b_j\rangle$ .
- Step 8: Step 8 has the following three sub-steps:
  - Step 1: For  $j = 0$  to  $2 \cdot i - 1$ :  
Reassign the names of the value stored in the location with the value  $|d_j\rangle$  to the name  $a_{n-2,i-j}$ .
  - Step 2: For  $j = i - 1$  to 1:  
Reassign the names of the value stored in the location with the value  $|b_j\rangle$  to the name  $b_j$ .
  - Reassign the names of the values stored in the locations  $|z\rangle$  to the name  $z$ .

4.3 Part 3: Remainder Restoration

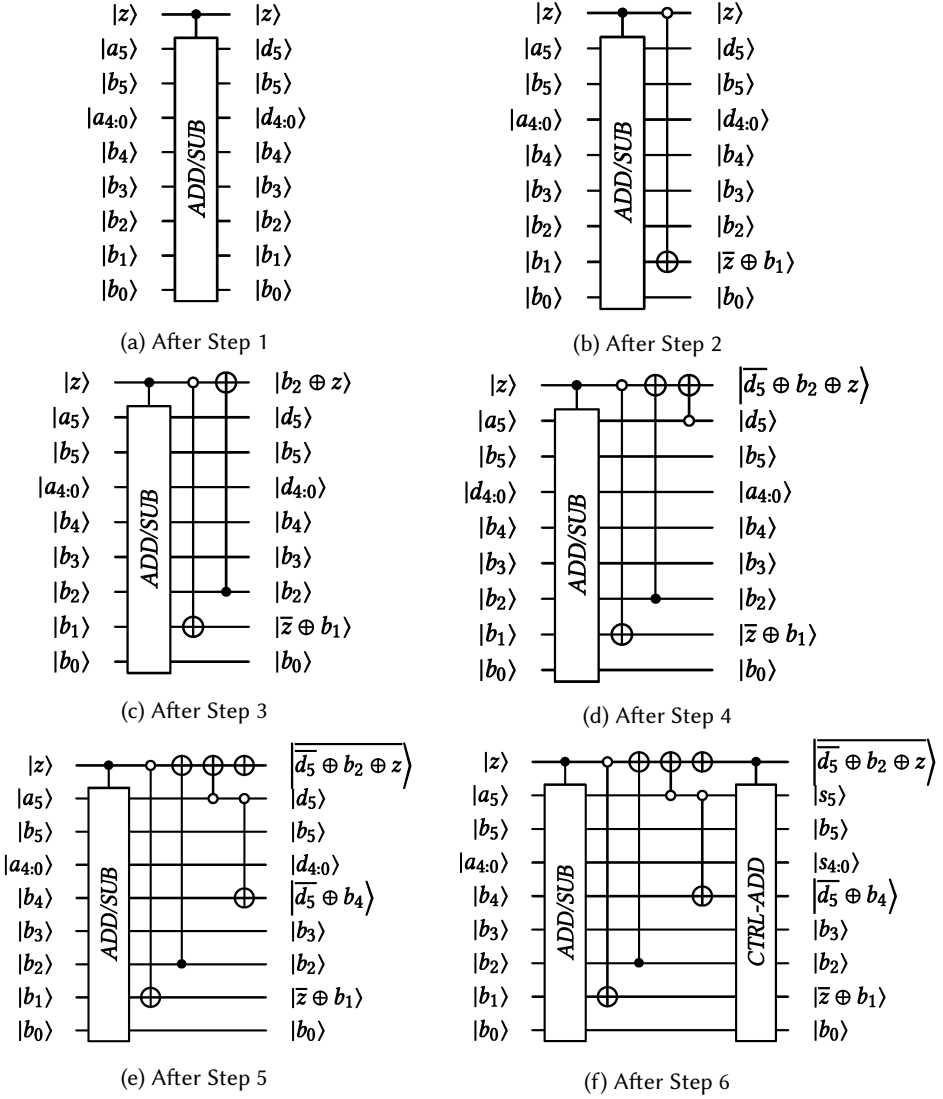


Fig. 10. Circuit generation of Part 3 of the proposed quantum square root circuit: Steps 1-6.

This Part is only repeated once. There are 9 Steps in this Part.

- Step 1: Step 1 has two sub-steps.
  - Step 1: For  $j = 0$  to  $n - 1$ :
    - At pair of locations  $|b_j\rangle$  and  $|a_j\rangle$  apply the quantum *ADD/SUB* circuit such that location  $|b_j\rangle$  will maintain the same value while location  $|a_j\rangle$  transforms two the sum or difference bit  $|d_j\rangle$
  - Step 2: At location  $|z\rangle$  apply the quantum *ADD/SUB* circuit such that the operation of the circuit will be conditioned on the value at location  $|z\rangle$ .

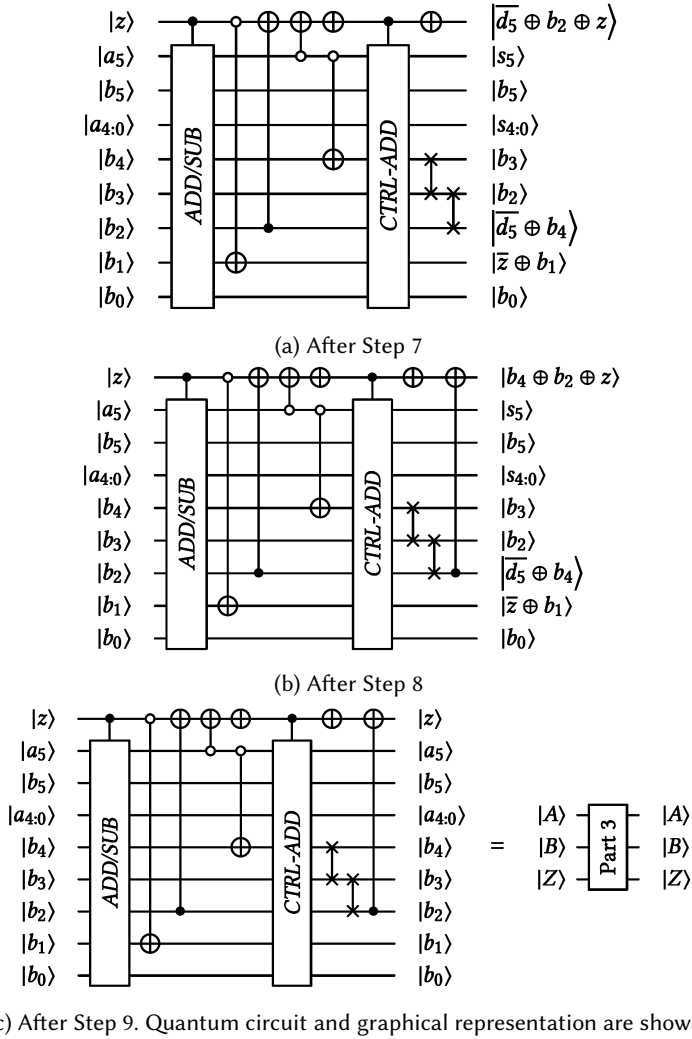


Fig. 11. Circuit generation of Part 3 of the proposed quantum square root circuit: Steps 7-9.

- Step 2: At locations  $|z\rangle$  and  $|b_1\rangle$  apply an inverted control CNOT gate such that location  $|z\rangle$  will maintain the same value while location  $|b_1\rangle$  transforms to the value  $|\bar{z} \oplus b_1\rangle$
- Step 3: At locations  $|b_2\rangle$  and  $|z\rangle$  apply a CNOT gate such that location  $|b_2\rangle$  will maintain the same value while location  $|z\rangle$  transforms to the value  $|b_2 \oplus z\rangle$
- Step 4: At locations  $|a_{n-1}\rangle$  and  $|z\rangle$  apply an inverted control CNOT gate such that location  $|b_2\rangle$  will maintain the same value while location  $|z\rangle$  transforms to the value  $|\overline{d_{n-1}} \oplus b_2 \oplus z\rangle$
- Step 5: Step 5 has two sub-steps.

- Step 1: At locations  $|a_{n-1}\rangle$  and  $|b_{\frac{n}{2}+1}\rangle$  apply an inverted control CNOT gate such that location  $|a_{n-1}\rangle$  will maintain the same value while location  $|b_{\frac{n}{2}+1}\rangle$  transforms to the value  $|d_{n-1} \oplus b_{\frac{n}{2}+1}\rangle$
- Step 2: At location apply  $|z\rangle$  apply a quantum NOT gate such that the location  $|z\rangle$  transforms to the value  $|\overline{d_{n-1} \oplus b_2 \oplus z}\rangle$
- Step 6: This Step has the following two sub-steps.
  - Step 1: At location  $|z\rangle$  apply a quantum conditional addition (*CTRL-ADD*) circuit such that the operation of the quantum *CTRL-ADD* circuit is conditioned on the value at location  $|z\rangle$ .
  - Step 2: For  $i = 0$  to  $n - 1$ :  
At pair of locations  $|a_i\rangle$  and  $|b_i\rangle$  apply the quantum *CTRL-ADD* circuit such that location  $|b_i\rangle$  will maintain the same value while location  $|a_i\rangle$  is transformed to the sum bit  $|s_i\rangle$ .
- Step 7: This Step has the following two sub-steps.
  - Step 1: At location  $|z\rangle$  apply a quantum NOT gate such that the location  $|z\rangle$  transforms to the value  $|\overline{d_{n-1} \oplus b_2 \oplus z}\rangle$ .
  - Step 2: For  $i = \frac{n}{2} + 1$  to 3:  
At locations  $|b_i\rangle$  and  $|b_{i-1}\rangle$  apply a quantum SWAP gate such that location  $|b_i\rangle$  will have the value at location  $|b_{i-1}\rangle$  and location  $|b_{i-1}\rangle$  will have the value at location  $|b_i\rangle$ .
- Step 8: At locations  $|b_2\rangle$  and  $|z\rangle$  apply a CNOT gate such that location  $|b_2\rangle$  will maintain the same value while location  $|z\rangle$  transforms to the value  $|\overline{d_{n-1} \oplus z}\rangle$
- Step 9: Step 9 has the following three sub-steps:
  - Step 1: For  $j = 0$  to  $n - 1$ :  
Reassign the names of the value stored in the location with the value  $|d_j\rangle$  to the name  $a_j$ .
  - Step 2: For  $j = 0$  to  $n - 1$ :  
Reassign the names of the value stored in the location with the value  $|b_j\rangle$  to the name  $b_j$ .
  - Reassign the name of the value stored in location  $|z\rangle$  to the name  $z$ .

## 5 PROOF OF CORRECTNESS

**Theorem:** Given a 2's compliment positive binary number  $a$  of even length  $n$  at location  $|a\rangle$ , a length  $n$  binary representation of 1 at location  $|b\rangle$  and a qubit  $|z\rangle$  where  $z = 0$ , then the proposed design methodology generates a quantum square root circuit that works correctly. The square root of  $a$  is at the location  $|b\rangle$ , the remainder from taking the square root of  $a$  is at location  $|a\rangle$  and qubit  $|z\rangle$  remains 0.

**Proof:** The proposed design methodology will make the following changes on the inputs.

### 5.1 Part 1: Initial Subtraction

Step 1 transforms the input states to:

$$|z\rangle \left| \sqrt{a_{\frac{n}{2}-1}} \right\rangle |d_0\rangle \left( \bigotimes_{j=0}^{n-3} |a_j\rangle \right) \left( \bigotimes_{j=0}^{n-1} |b_j\rangle \right) \quad (1)$$

After Steps 2 through 4, the input states  $|z\rangle$  and  $|a\rangle$  are transformed to:

$$\left| \sqrt{a_{\frac{n}{2}-1}} \oplus z \right\rangle \left| \sqrt{a_{\frac{n}{2}-1}} \right\rangle |d_0\rangle \left( \bigotimes_{j=0}^{n-3} |a_j\rangle \right) \quad (2)$$

After Steps 2 through 4, the input state  $|b\rangle$  is transformed to:

$$\left( \bigotimes_{j=3}^{n-1} |b_j\rangle \right) \left| \sqrt{a_{\frac{n}{2}-1}} \right\rangle \left| \sqrt{a_{\frac{n}{2}-1}} \oplus b_1 \right\rangle |b_0\rangle \quad (3)$$

Step 5 does not change the input states.

## 5.2 Part 2: Conditional Addition Subtraction

This Part is repeated  $\frac{n}{2} - 2$  times. For  $i = 2$  to  $\frac{n}{2} - 1$ :

The  $i$ th iteration of Step 1 transforms the input states  $|z\rangle$  and  $|a\rangle$  to:

$$\left| \sqrt{a_{\frac{n}{2}-i+1}} \oplus z \right\rangle \left| \sqrt{a_{\frac{n}{2}-i}} \right\rangle \left( \bigotimes_{j=n-2\cdot i}^{n-2} |d_j\rangle \right) \left( \bigotimes_{j=0}^{n-1-2\cdot i} |a_j\rangle \right) \quad (4)$$

The  $i$ th iteration of Step 1 transforms the input state  $|b\rangle$  to:

$$\left( \bigotimes_{j=i+1}^{n-1} |b_j\rangle \right) \left( \bigotimes_{j=2}^i \left| \sqrt{a_{\frac{n}{2}+j-i-1}} \right\rangle \right) |b_1\rangle |b_0\rangle \quad (5)$$

After the  $i$ th iteration of Steps 2 through 3, the input states  $|z\rangle$  and  $|a\rangle$  are transformed to:

$$|z\rangle \left| \sqrt{a_{\frac{n}{2}-i}} \right\rangle \left( \bigotimes_{j=n-2\cdot i}^{n-2} |d_j\rangle \right) \left( \bigotimes_{j=0}^{n-1-2\cdot i} |a_j\rangle \right) \quad (6)$$

After the  $i$ th iteration of Steps 2 through 3, the input state  $|b\rangle$  is transformed to:

$$\left( \bigotimes_{j=i+2}^{n-1} |b_j\rangle \right) \left| \sqrt{a_{\frac{n}{2}-i}} \right\rangle \left( \bigotimes_{j=2}^i \left| \sqrt{a_{\frac{n}{2}+j-i-1}} \right\rangle \right) |b_1\rangle |b_0\rangle \quad (7)$$

After the  $i$ th iteration of Steps 4 through 7, the input states  $|z\rangle$  and  $|a\rangle$  are transformed to:

$$\left| \sqrt{a_{\frac{n}{2}-i}} \oplus z \right\rangle \left| \sqrt{a_{\frac{n}{2}-i}} \right\rangle \left( \bigotimes_{j=n-2\cdot i}^{n-2} |d_j\rangle \right) \left( \bigotimes_{j=0}^{n-1-2\cdot i} |a_j\rangle \right) \quad (8)$$

After the  $i$ th iteration of Steps 4 through 7, the input state  $|b\rangle$  is transformed to:

$$\left( \bigotimes_{j=i+2}^{n-1} |b_j\rangle \right) \left( \bigotimes_{j=2}^{i+1} \left| \sqrt{a_{\frac{n}{2}+j-i-2}} \right\rangle \right) |b_1\rangle |b_0\rangle \quad (9)$$

The  $i$ th iteration of Step 8 does not change the input states.

### 5.3 Part 3: Remainder Restoration

Steps 1 through 3 of this Part are identical to Steps 1 through 3 of Part 2: Conditional Addition Subtraction. Thus, after Step 3, the input states  $|z\rangle$  and  $|a\rangle$  are transformed to:

$$|z\rangle |\sqrt{a_0}\rangle \left( \bigotimes_{j=0}^{n-2} |d_j\rangle \right) \quad (10)$$

After Step 3, the input state  $|b\rangle$  is transformed to:

$$\left( \bigotimes_{j=\frac{n}{2}+1}^{n-1} |b_j\rangle \right) |\sqrt{a_1}\rangle \left( \bigotimes_{j=2}^{\frac{n}{2}-1} |\sqrt{a_j}\rangle \right) |b_1\rangle |b_0\rangle \quad (11)$$

Thus, after Steps 4 and 5, the input states  $|z\rangle$  and  $|a\rangle$  are transformed to:

$$|\sqrt{a_0 \oplus z}\rangle |\sqrt{a_0}\rangle \left( \bigotimes_{j=0}^{n-2} |d_j\rangle \right) \quad (12)$$

After Steps 4 and 5, the input state  $|b\rangle$  is transformed to:

$$\left( \bigotimes_{j=\frac{n}{2}+2}^{n-1} |b_j\rangle \right) |\sqrt{a_0}\rangle \left( \bigotimes_{j=2}^{\frac{n}{2}} |\sqrt{a_{j-1}}\rangle \right) |b_1\rangle |b_0\rangle \quad (13)$$

Step 6 transforms the input states to:

$$|\sqrt{a_0 \oplus z}\rangle \left( \bigotimes_{j=0}^{n-1} |s_j\rangle \right) \left( \bigotimes_{j=\frac{n}{2}+2}^{n-1} |b_j\rangle \right) |\sqrt{a_0}\rangle \left( \bigotimes_{j=2}^{\frac{n}{2}} \sqrt{a_{j-1}} \right) |b_1\rangle |b_0\rangle \quad (14)$$

After Steps 7 and 8, the input states are transformed to:

$$|z\rangle \left( \bigotimes_{j=0}^{n-1} |r_j\rangle \right) \left( \bigotimes_{j=\frac{n}{2}+2}^{n-1} |b_j\rangle \right) \left( \bigotimes_{j=2}^{\frac{n}{2}+1} |\sqrt{a_{j-2}}\rangle \right) |b_1\rangle |b_0\rangle \quad (15)$$

Step 9 does not change the input states.

Thus, square root of  $a$  is at location  $|b\rangle$  and the remainder of calculating the square root of  $a$  is at location  $|a\rangle$ . The locations  $|z\rangle$ ,  $|b_{n-1:\frac{n}{2}+2}\rangle$  and  $|b_{1:0}\rangle$  are restored to their initial values. Thus, the proposed design methodology generates an quantum square root circuit that is functionally correct.

## 6 COST ANALYSIS

### 6.1 T Gate Cost

The T-count of the proposed quantum square root circuit is illustrated shortly for each Part of the proposed design.

#### 6.1.1 Part 1: Initial Subtraction.

- The T-count for Step 1 is 14. We use a quantum subtractor of T-count  $14 \cdot n - 14$  in this Step.
- Steps 2 through 5 do not require T-gates.

6.1.2 *Part 2: Conditional Addition or Subtraction.* The steps in this part are repeated  $\frac{n}{2} - 2$  times. For  $i = 2$  to  $\frac{n}{2} - 1$ :

- The T-count for the  $i$ th iteration of Step 1 is  $28 \cdot i - 14$ . We use a quantum *ADD/SUB* circuit of T-count  $14 \cdot n - 14$  in this Step.
- The  $i$ th iteration of 2 through 8 do not require T-gates.

6.1.3 *Part 3: Remainder Restoration.*

- The T-count for Step 1 is  $14 \cdot n - 14$ . We use a quantum *ADD/SUB* circuit of T-count  $14 \cdot n - 14$  in this Step.
- Steps 2 through 5 do not require T-gates.
- The T-count for Step 6 is  $21 \cdot n - 14$ . We use a quantum *CTRL-ADD* circuit of T-count  $21 \cdot n - 14$  in this Step.
- Steps 7 through 9 do not require T-gates.

Thus, The total T-count for the proposed quantum square root circuit is given as:

$$\left( \sum_{i=1}^{\frac{n}{2}} 28 \cdot i - 14 \right) + 21 \cdot n - 14 \quad (16)$$

The expression for the T-count (expression 16) can be simplified into the following expression:

$$\frac{7}{2} \cdot n^2 + 21 \cdot n - 14 \quad (17)$$

Table 2. Comparison of quantum square root circuits

	1	2	3	4	Proposed
T-count	$7 \cdot n^2 + 14 \cdot n$	$420 \cdot n^2 + 126 \cdot n - 196$	$\frac{21}{4} \cdot n^2 + \frac{105}{2} \cdot n - 42$	$\frac{21}{4} \cdot n^2 + \frac{7}{2} \cdot n - 14$	$\frac{7}{2} \cdot n^2 + 21 \cdot n - 14$
qubits	$\frac{1}{4} \cdot n^2 + 6 \cdot n - 2$	$\approx 42 \cdot n + 10$	$\approx \frac{1}{2}n^2 + 7 \cdot n + 2$	$\approx \frac{1}{2}n^2 + 3 \cdot n + 4$	$2 \cdot n + 1$

1 is the design by Sultana et. al. [21]

2 is the design by Bhaskar et. al. [6]

3 is the first design by AnanthaLakshmi et. al. [3]

4 is the second design by AnanthaLakshmi et. al. [3]

## 6.2 Cost Comparison

The comparison of the proposed quantum square root circuit with the current state of the art are illustrated in tables 2, 3 and 4. To compare our proposed square root circuit against the existing designs by Sultana et. al.[21] and AnanthaLakshmi et. al. [3], we implemented the designs with Clifford+T gates. We also apply the Bennett's garbage removal scheme (see [5]) to remove the garbage output from the designs by Sultana et. al. and AnanthaLakshmi et. al.. The total qubit cost values we use for each design by AnanthaLakshmi et. al. are estimates. The estimated qubit cost totals are calculated by summing the garbage output produced by the controlled subtraction circuits and the circuit outputs. AnanthaLakshmi et. al. indicated that outputs such as difference bits from the controlled subtraction circuits may be regarded as garbage output. However, the number of these additional outputs treated as garbage appears ad. hoc. in nature. Thus, the resulting qubit cost totals used in this work represent a lower bound of the number of qubits required by the square root designs by AnanthaLakshmi et. al..

To compare our proposed square root circuit against the existing design by Bhaskar et. al.[6], we implemented the design with Clifford+T gates. The square root design in Bhaskar et. al. requires



Table 3. Qubit cost comparison of quantum square root circuits

qubits	1	2	3	4	Proposed	% Impr w.r.t 1	% Impr w.r.t 2	% Impr w.r.t 3	% Impr w.r.t 4
4	26	≈ 178	≈ 38	≈ 24	9	65.38	≈ 94.94	≈ 76.32	≈ 62.50
8	62	≈ 346	≈ 90	≈ 60	17	72.58	≈ 95.09	≈ 81.11	≈ 71.67
16	158	≈ 682	≈ 242	≈ 180	33	79.11	≈ 95.16	≈ 86.36	≈ 81.67
32	446	≈ 1354	≈ 738	≈ 612	65	85.43	≈ 95.20	≈ 91.19	≈ 89.38
64	1406	≈ 2698	≈ 2498	≈ 2244	129	90.83	≈ 95.22	≈ 94.84	≈ 94.25
128	4862	≈ 5386	≈ 9090	≈ 8580	257	94.71	≈ 95.23	≈ 97.17	≈ 97.00
256	17918	≈ 10762	≈ 34562	≈ 33540	513	97.14	≈ 95.23	≈ 98.52	≈ 98.47
512	68606	≈ 21514	≈ 134658	≈ 132612	1025	98.51	≈ 95.24	≈ 99.24	≈ 99.23
Average:						85.46	≈ 95.16	≈ 90.59	≈ 86.77

1 is the design by Sultana et. al. [21]

2 is the design by Bhaskar et. al. [6]

3 is the first design by AnanthaLakshmi et. al. [3]

4 is the second design by AnanthaLakshmi et. al. [3]

Table 4. T-count comparison of quantum square root circuits

qubits	1	2	3	4	Proposed	% Impr w.r.t 1	% Impr w.r.t 2	% Impr w.r.t 3	% Impr w.r.t 4
4	168	6944	252	84	136	19.05	98.04	46.03	-
8	560	27776	714	350	388	30.71	98.60	45.66	-
16	2016	109760	2142	1386	1228	39.09	98.88	42.67	11.40
32	7616	435008	7014	5474	4252	44.17	99.02	39.38	22.32
64	29568	1730624	24822	21714	15676	46.98	99.09	36.85	27.81
128	116480	6902336	92694	86450	60028	48.46	99.13	35.24	30.56
256	462336	27567680	357462	344946	234748	49.23	99.15	34.33	31.95
512	1842176	110186048	1403094	1378034	928252	49.61	99.16	33.84	32.64
Average:						40.91	98.88	39.25	26.11

1 is the design by Sultana et. al. [21]

2 is the design by Bhaskar et. al. [6]

3 is the first design by AnanthaLakshmi et. al. [3]

4 is the second design by AnanthaLakshmi et. al. [3]

$5 \cdot \lceil \log_2(b) \rceil$  multiplications and  $3 \cdot \lceil \log_2(b) \rceil$  additions (where  $b$  is the accuracy of the solution). We use an implementation that has the lowest possible solution accuracy and thus let  $b = 4$ . This is because the T gate and qubit costs increases as a function of solution accuracy. Thus, the square root circuit based on the design by Bhaskar et. al. requires 10 multiplications and 6 additions. Bhaskar et. al. did not specify a quantum adder or multiplier design for use in their square root quantum circuit design. Therefore, to have a fair comparison against our work we use a quantum adder that has a T-count of  $14 \cdot n - 14$ , a qubit cost of  $2 \cdot n + 1$  and produces no garbage output. Further, we use a quantum multiplier that has a T-count of  $21 \cdot n^2 - 14$ , a qubit cost of  $4 \cdot n + 1$  and produces no garbage output. We assume that given two inputs on quantum registers  $|a\rangle$  and  $|b\rangle$ , the quantum multiplier will produce the product of  $|a\rangle$  and  $|b\rangle$  on  $2 \cdot n + 1$  ancillae. The inputs  $|a\rangle$  and  $|b\rangle$  will maintain the same value at the end of computation. Consequently, at the end of computation, the square root circuit based on the design by Bhaskar et. al. will have garbage

outputs. We apply the Bennett's garbage removal scheme to remove the garbage output from the quantum circuit implementation of the design by Bhaskar et. al.

Table 2 shows the T-count cost of the proposed quantum square root circuit and the designs by Sultana et. al., Bhaskar et. al. and AnanthaLakshmi et. al. are of order  $O(n^2)$ . Table 2 also shows that our proposed design and the design by Bhaskar et. al. have a qubit cost of order  $O(n)$  while the qubit cost for the designs by Sultana et. al. and AnanthaLakshmi et. al. are of order  $O(n^2)$ .

Table 3 shows that our proposed design methodology achieves improvement ratios ranging from 65.38% to 98.51%, 94.94% to 95.24%, 76.32% to 99.24% and 62.50% to 99.23 compared to the designs by Sultana et. al., Bhaskar et. al. and AnanthaLakshmi et. al. in terms of total qubits. Table 4 shows that the proposed design methodology achieves improvement ratios ranging from 19.05% to 49.61%, 98.04% to 99.16%, 33.84% to 46.03% and 0.00% to 32.64% compared to the designs by Sultana et. al., Bhaskar et. al. and AnanthaLakshmi et. al. in terms of T-count. Table 4 also illustrates that the circuit optimizations presented by AnanthaLakshmi et. al. are most effective for small values of  $n$ . We calculated that for  $n \geq 10$ , the proposed square root circuit requires fewer T gates than the optimized design presented by AnanthaLakshmi et. al..

## 7 CONCLUSION

In this work, we present a new design of a quantum square root circuit. The proposed design has zero overhead in terms of garbage outputs. The proposed design also requires fewer T gates and less qubits than the current state of the art. The proposed quantum square root circuit has been functionally verified by formal proof and by functional simulation in Verilog. The proposed quantum square root circuit could form a crucial component in the quantum hardware implementations of scientific algorithms where qubits and T-count are of primary concern.

## REFERENCES

- [1] M. Amy, D. Maslov, and M. Mosca. 2014. Polynomial-Time T-Depth Optimization of Clifford+T Circuits Via Matroid Partitioning. *IEEE Transactions on Computer-Aided Design of Integrated Circuits and Systems* 33, 10 (Oct 2014), 1476–1489. <https://doi.org/10.1109/TCAD.2014.2341953>
- [2] M. Amy, D. Maslov, M. Mosca, and M. Roetteler. 2013. A Meet-in-the-Middle Algorithm for Fast Synthesis of Depth-Optimal Quantum Circuits. *IEEE Transactions on Computer-Aided Design of Integrated Circuits and Systems* 32, 6 (June 2013), 818–830. <https://doi.org/10.1109/TCAD.2013.2244643>
- [3] A.V. AnanthaLakshmi and Gnanou Florence Sudha. 2017. A novel power efficient 0.64-GFlops fused 32-bit reversible floating point arithmetic unit architecture for digital signal processing applications. *Microprocessors and Microsystems* 51, Supplement C (2017), 366 – 385. <https://doi.org/10.1016/j.micpro.2017.01.002>
- [4] S Beaugard. 2003. Circuit for Shor's algorithm using  $2n+3$  qubits. *QUANTUM INFORMATION & COMPUTATION* 3, 2 (MAR 2003), 175–185.
- [5] C. H. Bennett. 1973. Logical Reversibility of Computation. *IBM J. Res. Dev.* 17, 6 (Nov. 1973), 525–532. <https://doi.org/10.1147/rd.176.0525>
- [6] M. K. Bhaskar, S. Hadfield, A. Papageorgiou, and I. Petras. 2016. Quantum Algorithms and Circuits for Scientific Computing. *QUANTUM INFORMATION & COMPUTATION* 16, 3-4 (MARCH 2016), 197–236.
- [7] Donny Cheung, Dmitri Maslov, Jimson Mathew, and Dhiraj K. Pradhan. 2008. *Theory of Quantum Computation, Communication, and Cryptography: Third Workshop, TQC 2008 Tokyo, Japan, January 30 - February 1, 2008. Revised Selected Papers*. Springer Berlin Heidelberg, Berlin, Heidelberg, Chapter On the Design and Optimization of a Quantum Polynomial-Time Attack on Elliptic Curve Cryptography, 96–104.
- [8] S. J. Devitt, A. M. Stephens, W. J. Munro, and K. Nemoto. 2013. Requirements for fault-tolerant factoring on an atom-optics quantum computer. *Nature Communications* 4, Article 2524 (Oct. 2013), 2524 pages. <https://doi.org/10.1038/ncomms3524> arXiv:quant-ph/1212.4934
- [9] Peter Selinger et. al. 2016. *The Quipper System*. Available at: <http://www.mathstat.dal.ca/~selinger/quipper/doc/>.
- [10] David Gosset, Vadym Kliuchnikov, Michele Mosca, and Vincent Russo. 2014. An algorithm for the T-count. *Quantum Information & Computation* 14, 15-16 (2014), 1261–1276. <http://www.rintonpress.com/xxqic14/qic-14-1516/1261-1276.pdf>
- [11] IBM. 2017. *Quantum Computing - IBM Q*. Available at: <https://www.research.ibm.com/ibm-q/>.

- [12] N. Cody Jones, Rodney Van Meter, Austin G. Fowler, Peter L. McMahon, Jungsang Kim, Thaddeus D. Ladd, and Yoshihisa Yamamoto. 2012. Layered Architecture for Quantum Computing. *Phys. Rev. X* 2 (Jul 2012), 031007. Issue 3. <https://doi.org/10.1103/PhysRevX.2.031007>
- [13] Igor L. Markov and Mehdi Saeedi. 2012. Constant-optimized quantum circuits for modular multiplication and exponentiation. *Quantum Information & Computation* 12, 5-6 (2012), 361–394. <http://www.rintonpress.com/xxqic12/qic-12-56/0361-0394.pdf>
- [14] D. Michael Miller, Mathias Soeken, and Rolf Drechsler. 2014. Mapping NCV Circuits to Optimized Clifford+T Circuits. In *Reversible Computation*, Shigeru Yamashita and Shin-ichi Minato (Eds.). Lecture Notes in Computer Science, Vol. 8507. Springer International Publishing, 163–175.
- [15] C. Monroe, R. Raussendorf, A. Ruthven, K. R. Brown, P. Maunz, L.-M. Duan, and J. Kim. 2014. Large-scale modular quantum-computer architecture with atomic memory and photonic interconnects. *Phys. Rev. A* 89 (Feb 2014), 022317. Issue 2. <https://doi.org/10.1103/PhysRevA.89.022317>
- [16] A. Montanaro. 2014. Quantum pattern matching fast on average. *ArXiv e-prints* (Aug. 2014). arXiv:quant-ph/1408.1816
- [17] A. Paler and S. J. Devitt. 2015. An introduction into fault-tolerant quantum computing. In *2015 52nd ACM/EDAC/IEEE Design Automation Conference (DAC)*. 1–6. <https://doi.org/10.1145/2744769.2747911>
- [18] Alexandru Paler, Ilia Polian, Kae Nemoto, and Simon J Devitt. 2017. Fault-tolerant, high-level quantum circuits: form, compilation and description. *Quantum Science and Technology* 2, 2 (2017), 025003. <http://stacks.iop.org/2058-9565/2/i=2/a=025003>
- [19] I. Polian and A. G. Fowler. 2015. Design automation challenges for scalable quantum architectures. In *2015 52nd ACM/EDAC/IEEE Design Automation Conference (DAC)*. 1–6. <https://doi.org/10.1145/2744769.2747921>
- [20] J Proos and C Zalka. 2003. Shor’s discrete logarithm quantum algorithm for elliptic curves. *QUANTUM INFORMATION & COMPUTATION* 3, 4 (JUL 2003), 317–344.
- [21] S. Sultana and K. Radecka. 2011. Reversible implementation of square-root circuit. In *2011 18th IEEE International Conference on Electronics, Circuits, and Systems*. 141–144. <https://doi.org/10.1109/ICECS.2011.6122234>
- [22] Himanshu Thapliyal. 2016. Mapping of subtractor and adder-subtractor circuits on reversible quantum gates. In *Transactions on Computational Science XXVII*. Springer, 10–34.
- [23] W. van Dam and G. Seroussi. 2002. Efficient Quantum Algorithms for Estimating Gauss Sums. *eprint arXiv:quant-ph/0207131* (July 2002). arXiv:quant-ph/0207131
- [24] Wim van Dam and Igor E. Shparlinski. 2008. *Classical and Quantum Algorithms for Exponential Congruences*. Springer Berlin Heidelberg, Berlin, Heidelberg, 1–10.
- [25] Paul Webster, Stephen D. Bartlett, and David Poulin. 2015. Reducing the overhead for quantum computation when noise is biased. *Phys. Rev. A* 92 (Dec 2015), 062309. Issue 6. <https://doi.org/10.1103/PhysRevA.92.062309>
- [26] Xinlan Zhou, Debbie W. Leung, and Isaac L. Chuang. 2000. Methodology for quantum logic gate construction. *Phys. Rev. A* 62 (Oct 2000), 052316. Issue 5. <https://doi.org/10.1103/PhysRevA.62.052316>
- [27] Xinlan Zhou, Debbie W. Leung, and Isaac L. Chuang. 2000. Methodology for quantum logic gate construction. *Phys. Rev. A* 62 (Oct 2000), 052316. Issue 5. <https://doi.org/10.1103/PhysRevA.62.052316>

Received February 2007; revised March 2009; accepted June 2009